

# Enhancement of $T_c$ by point-like disorder and anisotropic gap in FeSe

S. Teknowijoyo,<sup>1</sup> K. Cho,<sup>1</sup> M. A. Tanatar,<sup>1</sup> J. Gonzales,<sup>1</sup> A. E. Böhmer,<sup>1</sup> O. Cavani,<sup>2</sup>  
V. Mishra,<sup>3,4</sup> P. J. Hirschfeld,<sup>5</sup> S. L. Bud'ko,<sup>1</sup> P. C. Canfield,<sup>1</sup> and R. Prozorov<sup>1,\*</sup>

<sup>1</sup>*Ames Laboratory and Department of Physics & Astronomy, Iowa State University, Ames, IA 50011, USA*

<sup>2</sup>*Laboratoire des Solides Irradiés, École Polytechnique, CNRS,  
CEA, Université Paris-Saclay, 91128 Palaiseau Cedex, France*

<sup>3</sup>*Joint Institute of Computational Sciences, University of Tennessee, Knoxville, TN-37996, USA*

<sup>4</sup>*Center for Nanophase Materials Sciences, Oak Ridge National Laboratory, Oak Ridge, TN-37831, USA*

<sup>5</sup>*Department of Physics, University of Florida, Gainesville, Florida 32611, USA*

(Dated: 13 May 2016)

A highly anisotropic superconducting gap is found in single crystals of FeSe by studying the London penetration depth,  $\Delta\lambda$ , measured down to 50 mK in samples before and after 2.5 MeV electron irradiation. The gap minimum increases with introduced point - like disorder, indicating the absence of symmetry - imposed nodes. Surprisingly, the superconducting transition temperature,  $T_c$ , increases by 0.4 K from  $T_{c0} \approx 8.8$  K while the structural transition temperature,  $T_s$ , decreases by 0.9 K from  $T_{s0} \approx 91.2$  K after electron irradiation. We discuss several explanations for the  $T_c$  enhancement, and propose that local strengthening of the pair interaction by irradiation-induced Frenkel defects most likely explains the phenomenon.

## INTRODUCTION

Deliberately introduced point - like disorder may serve as a *phase - sensitive* tool to probe the superconducting gap structure and relative amplitudes of the pairing potential [1–6]. Usually, only the changes of the superconducting transition temperature,  $T_c$ , are studied. However, in complex materials, such as iron-based superconductors (IBS), this does not lead to unique predictions, see Ref. 6 and references therein. Therefore, simultaneous measurement of another disorder-sensitive parameter, for example, London penetration depth,  $\lambda(T)$ , can be used to impose additional constraints on the possible pairing models. Measurements of the low-temperature variation,  $\Delta\lambda(T) = \lambda(T) - \lambda(0)$ , can be used to study the gap anisotropy [7, 8] and to distinguish between  $s_{\pm}$  and  $s_{++}$  pairing [5]. The latter was successfully used to study nodal  $\text{BaFe}_2(\text{As,P})_2$  [9] and  $\text{SrFe}_2(\text{As,P})_2$  [7] where potential scattering lifted the nodes proving them accidental, therefore strongly supporting  $s_{\pm}$  pairing.

The majority of iron - based superconductors (IBS) have a region of coexisting superconductivity and long-range magnetic order (LRMO) in their temperature - composition phase diagram, usually at low doping levels. Whereas this leads to some very interesting physics [10–18], it complicates the analysis of the superconducting gap structure [4, 14, 19]. FeSe, on the other hand, only exhibits a structural transition around  $T_s \approx 90$  K, but no LRMO at the ambient pressure [20]. Being a nearly stoichiometric compound with relatively simple electronic band structure [21], FeSe offers a unique opportunity to study iron-based superconductivity without complications of LRMO and elevated scattering, which is always significant in charge - doped compounds [14, 22, 23]. The temperature-pressure phase diagram of FeSe is quite non-trivial. The superconducting transition tempera-

ture,  $T_c$ , is non-monotonic, – increasing initially up to 0.8 GPa, then decreasing, reaching a minimum at 1.3 GPa and increasing again [24–26]. Despite the absence of LRMO, a strong nematic response is found in FeSe, and has been discussed in terms of both spin and orbital fluctuations [27–31]. Additional interest in this material stems from the discovery of high temperature superconductivity with  $T_c \approx 65$  K in a single-layer FeSe grown on a  $\text{SrTiO}_3$  [32, 33], as well as the intriguing possibility of being in the regime of a crossover from Bose-Einstein condensation (BEC) and Bardeen-Cooper-Schrieffer (BCS) coupling due to small Fermi energies comparable to superconducting gap values [34, 35].

Most studies of IBS have converged on generalized  $s_{\pm}$  pairing as the basic and quite robust pairing mechanism supporting both nodeless and nodal states [17, 18]. In FeSe, anisotropic line nodes or deep minima were found theoretically [36–38]. Experimentally, scanning tunneling spectroscopy (STS) [39], London penetration depth and thermal conductivity [34] claimed nodal superconductivity. However, measurements of the lower critical field [40], low-temperature specific heat [41, 42], other STM [42] and other thermal conductivity studies [43, 44] are consistent with nodeless superconducting gap. A cross-over from nodal in the bulk to nodeless at the twin boundary is found from STS [45]. In all these studies, however, highly anisotropic gap and/or multi-band physics are present. On the other hand, a single large nodeless gap has been reported in single-layer FeSe [32, 46]. Despite the same chemical formula, this material also has a very different bandstructure and very different  $T_c$ , compared to the bulk FeSe. This, however, shows how susceptible this compound is to permutations of its chemical-physical state.

One possible scenario to reconcile these apparently contradictory results is to consider marginal, accidental

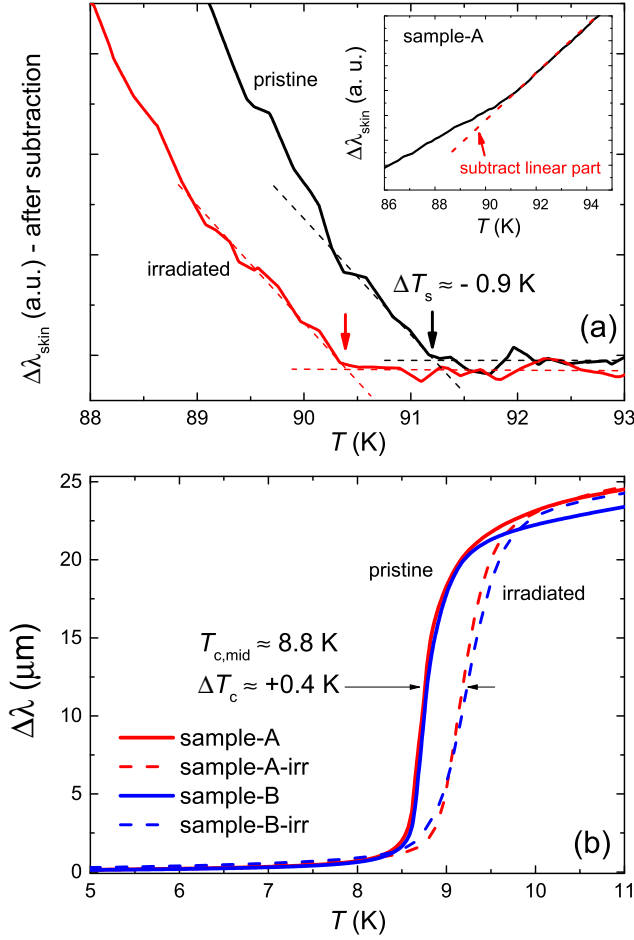


FIG. 1. (Color online) (a) Variation of normal state skin depth  $\Delta\lambda_{skin}(T \gg T_c)$  of sample A after linear-subtraction as shown in the *inset*. Arrows mark structural transition,  $T_s$ , before and after 2.5 MeV electron irradiation of  $1.8 \text{ C/cm}^2$ . (b) London penetration depth  $\Delta\lambda(T)$  before and after electron irradiation in Samples A and B.

nodes in the clean limit, which are lifted by the natural disorder always present to some degree in actual samples [44]. To probe this scenario, in this work the superconducting gap structure of vapor-transport grown FeSe crystals was studied by measuring the low-temperature variation of the London penetration depth,  $\Delta\lambda(T)$ , before and after 2.5 MeV electron irradiation. Using power-law fitting,  $\Delta\lambda(t) \sim t^n$ , ( $t \equiv T/T_c$ ), we find that the exponent  $n$  is much greater than the terminal dirty-limit value of 2 in all samples, signaling a nodeless gap. Irradiated samples show an even larger  $n$ , extending up to a higher temperature of the fitting range. Moreover, BCS-like fitting with gap magnitude as free parameter clearly shows an increase of the gap minimum upon introduction of point-like disorder. Both results are consistent with the smearing of the anisotropic part of the gap. Surprisingly, after  $1.1 \times 10^{19} \text{ e}^-/\text{cm}^2$  2.5 MeV electron irradiation,  $T_c$  has *increased* by 0.4 K from 8.8 K, while  $T_s$

decreased by 0.9 K from 91.2 K. These opposite trends are similar to the effect of pressure [25, 26, 47] and also imply that pair-breaking due to non-magnetic disorder is quite small. Overall, our results are consistent with highly anisotropic superconducting gap, which may have accidental nodes in the clean limit. While we cannot distinguish between generalized  $s_{\pm}$  and highly anisotropic multiband  $s_{++}$  pairing, we can limit the former to the case where intra-band pairing dominates the inter-band pairing.

Throughout the paper, we use the following terminology for multiband pairing:  $s_{++}$  is when the superconducting order parameters are of the same sign on different bands, and  $s_{\pm}$  when some are of the opposite sign. For the latter we distinguish between the case of dominant intraband pairing vs. dominant interband pairing, since these two cases respond very differently to nonmagnetic disorder. For a 2-band system with interaction potential  $V_{ij}$ , the former is realized when  $\langle V \rangle \equiv n_1(V_{11} + V_{12}) + n_2(V_{22} + V_{21}) > 0$ , where  $V_{11}$  and  $V_{22}$  are intraband, and  $V_{12}$  and  $V_{21}$  are inter-band pairing potentials and  $n_1 = N_1/N(0)$  and  $n_2 = 1 - n_1$  are the normalized partial densities of state (DOS) on two bands and  $N(0)$  is the total DOS [3]. We will call this state “intra-band”  $s_{\pm}$ . The second possibility,  $\langle V \rangle < 0$ , is “interband”  $s_{\pm}$ . It is important to note that even when  $\langle V \rangle > 0$ , the order parameters will have opposite signs and, thus, this is an  $s_{\pm}$  pairing state.

Finally, we note that the term s-wave pairing used throughout this paper refers to the state that has the full symmetry of the lattice just above the superconducting transition. In the case of FeSe, this is  $C_2$  rather than  $C_4$  due to the strong nematic symmetry breaking that occurs at the structural transition, and the Fermi surface that drives the superconducting gap function is strongly  $C_2$  symmetric according to ARPES. In terms of the harmonics of the tetragonal system, such a state would be described as an  $s + d$  state

## EXPERIMENTAL

Single crystals of FeSe were grown using a modified chemical vapor transport method [26, 48]. The variation of the in-plane London penetration depth,  $\Delta\lambda(T)$ , was measured using a self-oscillating tunnel-diode resonator (TDR) down to 50 mK [2, 14, 49]. The crystals under study have typical dimensions of about  $0.5 \times 0.5 \times 0.03 \text{ mm}^3$ . The samples were extensively characterized by measurements of magnetization, electric transport, Mössbauer spectroscopy and high energy x-ray scattering, including under pressure as described elsewhere [26, 31, 50].

The ratio of resistivities,  $RRR(300/10) \equiv \rho(300 \text{ K})/\rho(10 \text{ K}) \approx 20$ . A simple linear extrapolation to  $T = 0$ , gives  $RRR(300/0) \approx 125$ . In comparison, previous work

on vapor transport grown samples that found nodal superconductivity gives a very similar for  $RRR(300/10)$ , but results in a negative linear extrapolation, indicating lower residual resistivity,  $\rho(0)$ , hence a potentially less disordered sample [34].

To investigate the effect of deliberately introduced point - like disorder,  $\Delta\lambda(T)$  was measured before and after 2.5 MeV electron irradiation performed at the SIRIUS Pelletron facility of the Laboratoire des Solides Irradiés (LSI) at the École Polytechnique, France [51]. The acquired irradiation dose for our two irradiated samples was  $1.8 \text{ C/cm}^2$ . Here  $1 \text{ C/cm}^2 = 6.24 \times 10^{18} \text{ electrons/cm}^2$ . As shown in the *Supplementary Information* section, by calculating the Frenkel pairs (vacancy - interstitial) production cross-section we estimate creation of  $\sim 0.05 \text{ at.}\%$  of Frenkel pairs per Fe and per Se ( $0.1 \text{ at.}\%$  total pairs per formula or  $0.2 \text{ at.}\%$  per unit cell ( $Z=2$ )). Within the excellent sensitivity of the TDR technique, these defects are non-magnetic.

Three samples were measured. Samples A and B were measured before and after electron irradiation. Sample C was measured, cut in half and measured again to estimate the  $c$ -axis London penetration depth as described in Ref. 14.

## RESULTS

Figure 1 shows high temperature measurements to probe the effect of electron irradiation on  $T_c$  and  $T_s$ . In the normal state, the TDR signal is proportional to the normal skin depth,  $\lambda_{skin} \sim \sqrt{\rho}$  and the resistivity,  $\rho(T)$ , has a kink at  $T_s$  [31] which is detected here via  $\lambda_{skin}(T)$ . To visualize the transition, we subtract a linear part above  $T_s$  as shown in the *inset* in Fig. 1(a). The structural transition temperature,  $T_s$ , has shifted down by  $-0.9 \text{ K}$  in sample A after irradiation. Similar behavior was also observed for sample B. Figure 1(b) shows the region of superconducting transition. Both samples A and B show very similar behavior with  $T_c \approx 8.8 \text{ K}$  (mid-point) *increasing* by  $0.4 \text{ K}$ . Such increase is highly unusual and its observation imposes strict limitations on the structure of the superconducting order parameter. We note that although  $T_c$  enhancement reported here was measured in two different samples, we only had the opportunity to access one irradiation dose of  $1.8 \text{ C/cm}^2$ . Scenarios discussed in this paper may, in fact, lead to some non-monotonic behavior and further studies of  $T_s$  and  $T_c$  as function of irradiation dose are needed.

Figure 2 shows  $\Delta\lambda(t)$  of samples A and B before (solid lines) and after (dashed lines) 2.5 MeV electron irradiation dose of  $1.8 \text{ C/cm}^2$ . The penetration depth remains practically flat at  $T < 0.05T_c$ . Its amplitude increases faster with temperatures in irradiated samples, signaling an increase of the number of thermally excited quasiparticles compared to the pristine case. The inset shows

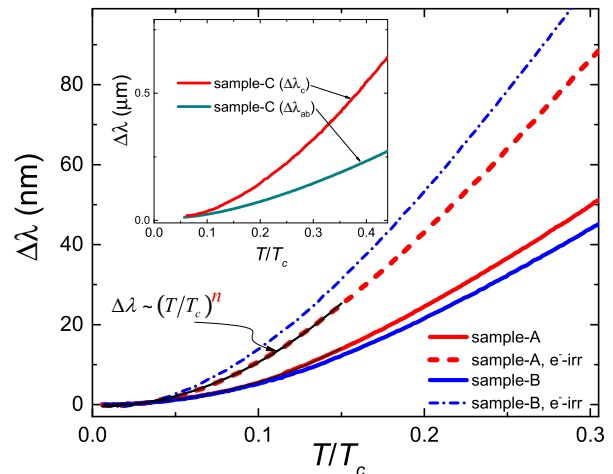


FIG. 2. (Color online) Low-temperature part of  $\Delta\lambda(t)$  of samples A (red) and B (blue) before (solid lines) and after (dashed lines) electron irradiation of  $1.8 \text{ C/cm}^2$ . *Inset* shows  $\Delta\lambda_{ab}$  (teal) and  $\Delta\lambda_c$  (red) of sample C.

in-plane, ( $\Delta\lambda_{ab}$ ), and out-of-plane, ( $\Delta\lambda_c$ ), penetration depths measured in sample C [14]. The ratio of  $\Delta\lambda_{ab}$  and  $\Delta\lambda_c$  at  $T = 0.3T_c$  is about 3, consistent with the relatively low anisotropy of other iron-based superconductors [14].

With an apparent saturation of  $\Delta\lambda(T)$  only at quite low temperatures, we analyze its behavior using two approaches. First, following our previous studies [14], we fit the London penetration depth by the power-law,  $\Delta\lambda(t) = At^n$ . The solid black curve, indicated by an arrow in Fig. 2, shows an example of such a fit. We examine the dependence of the exponent  $n$  on the upper limit of the fitting range,  $T_{max}/T_c$ , which was varied from  $0.05 T_c$  to  $0.3 T_c$  while the lower-limit was fixed as a base temperature of about  $50 \text{ mK}$ . Figure 3 shows how the exponent  $n$  increases with the decrease of  $T_{max}/T_c$  reaching the values significantly greater than 2 below  $0.1T_c$ . This indicates the presence of a small but finite gap, because both accidental and symmetry-imposed line nodes result in  $1 \leq n \leq 2$ .

As discussed above, STS experiments on high quality samples reported evidence for gap nodes in thin films [39] and single crystals [34], and from the theoretical standpoint, a ground state with very shallow  $C_2$ -symmetric nodes was found within spin fluctuation calculations with orbital ordering[37, 38], both in apparent contrast to our small gap result [52]. However, we know that accidental nodes can be lifted by intraband disorder scattering[53]. It may therefore be that our samples are slightly more disordered than those that show nodes. A similar suggestion was made in recent work on thermal conductivity [44].

It is also possible that samples of FeSe differ from one another not because of small differences in defect

concentrations, but due to different concentrations of twin boundaries due to growth conditions. Watashige *et al.* [45] have shown that even the bulk crystals exhibiting a nodal state show large scale regions of full gap behavior in the neighborhood of twin boundaries. Depending on its irregularity, the twin boundary may act a pair breaker, in which case this effect may be simply another version of the disorder node lifting phenomenon. The long range nature of the effect[45] suggests, however, that other physics may be in play. At present we cannot make convincing statements about the origin of our small gaps, but it appears clear that the gap is sensitive to small perturbations, which can gap a nodal state, and at present the most natural explanation seems to be that disorder is lifting the nodes in slightly less pure samples.

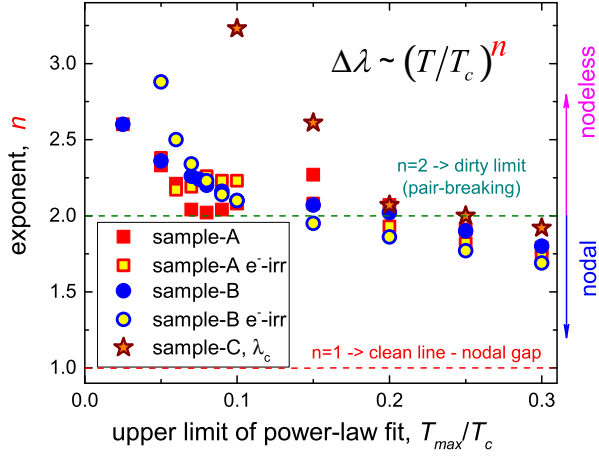


FIG. 3. (Color online) Exponent,  $n$ , of power-law fitting for data shown in Fig. 2. x-axis is the upper-limit of the fitting range. In all samples, the exponents increase well above dirty-limit of  $n=2$  at low-temperatures, indicating the presence of small, but finite superconducting gap. After electron irradiation,  $n$  becomes even higher, probably signaling some reduction of the gap anisotropy. The  $c$ -axis direction is also gapped.

Our second approach to analyze low-temperature behavior is to use BCS single gap fit,  $\Delta\lambda = C_1 + C_2\sqrt{\pi\delta/2t}\exp(-\delta/t)$  with variable upper temperature limit,  $T_{max}/T_c$ , free parameters  $C_1$  and  $C_2$ , and the value of the gap,  $\delta = \Delta(0)/T_c$  also as a free parameter. This procedure can be used to estimate the minimum gap in the system, provided that the measurements were done down to low enough temperature, which is the case here. Figure 4(a) shows one example of the exponential fitting of the sample B data before and after electron irradiation. Figure 4(b) presents the ratio of  $\Delta(0)/T_c$  obtained as the best fit parameter for several values of the upper limit of the fitting range. While there is only a hint of saturation in the pristine curve, the irradiated fits saturate at about  $\Delta_{min}(0)/T_c$  indicating a truly exponential behavior. In addition, we see that the smaller range fits indicate clearly that the minimum gap has increased upon ir-

radiation, a phenomenon analogous to node lifting, which results from the averaging of the gap anisotropy by intra-band disorder[53]. This is only possible if the anisotropy, and possible nodes, are not imposed by the pairing potential symmetry (i.e., anisotropic  $s$ -wave or  $s_{\pm}$ , but not  $d$ -wave).

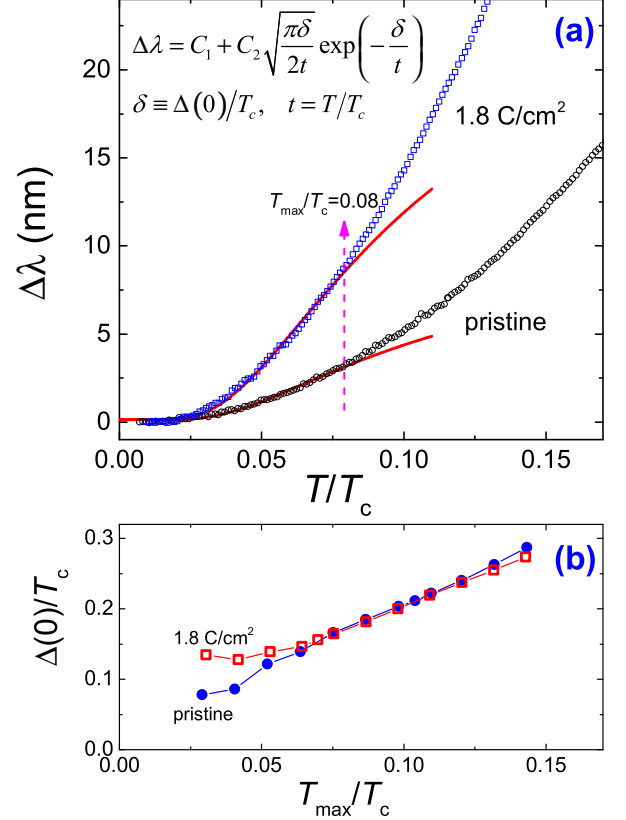


FIG. 4. (Color online) (a) low temperature  $\Delta\lambda(t)$  and example of BCS - like fitting of data for sample B for  $T_{max}/T_c \approx 0.08$  before (lower curve) and after  $1.8 \text{ C/cm}^2$  electron irradiation (upper curve). Also shown an equation and definitions used. (b)  $\Delta(0)/T_c$  ratio obtained as a best fit parameter with different upper limits of the fitting range.

To gain further insight into the gap structure, we need to analyze the temperature-dependent superfluid density,  $\rho_s = (1 + \Delta\lambda(T)/\lambda(0))^{-2}$ , over the entire temperature interval. Our TDR technique only measured  $\Delta\lambda(T)$  and we need to know the absolute value of the London penetration depth,  $\lambda(0)$ . In Fig. 5, the superfluid density  $\rho_s(t)$  is plotted with  $\lambda(0) = 400 \text{ nm}$  obtained from microwave cavity perturbation measurements of similar FeSe crystals [34] and with  $\lambda(0) = 330 \text{ nm}$ , obtained from the best fit to the anisotropic order parameter described in the following paragraph. The curves are not too far from each other, so there is no substantial difference for the choice of  $\lambda(0)$  in this spatial range. Superfluid densities for both samples A and B before and after electron irradiation are shown in Fig. S2. Note that both are normalized arbitrarily to 1 at  $T = 0$ . While it is clear that electron

irradiation results in a suppressed superfluid density at all temperatures, we cannot make more rigorous conclusions, because  $\lambda(0)$  definitely increases with disorder, but at the moment we do not know how much.

To describe the data over the whole temperature range, we discuss fits using a single anisotropic order parameter, as well as two isotropic gaps. Neither is really appropriate for a multiband, anisotropic superconductor, but these analyses can give some sense of what properties the true gap function must display. In order to analyze the data with an anisotropic order parameter with the possibility of both gapped and nodal states, we use a convenient parameterization,  $\Delta(t, \phi) = \Psi(t)\Omega(\phi)$ , where the temperature - dependent part,  $\Psi(t)$ , is obtained from the self-consistency equation [22] and the angular part,  $\Omega(\phi) = (1 + r \cos(4\phi))/(1 + r^2/2)^{1/2}$ , is chosen for a simple representation of the gap anisotropy. Here  $t = T/T_c$ . In general, one could choose other anisotropic harmonics, e.g.  $\sim \cos(n\phi)$  with the symmetry of the lattice[16, 18], but this would not alter the qualitative results. The angular part is normalized,  $\langle \Omega^2 \rangle = 1$ . More details are given in *Supplementary Information*. A direct fit of the experimental  $\rho_s(t)$  with  $\lambda(0) = 400$  nm to this anisotropic gap can only reproduce the data roughly below  $0.3T/T_c$  with  $r = 0.70$ . However, a small adjustment of  $\lambda(0)$  to 330 nm, produces a curve that can be fitted with  $r = 0.75$  in the whole temperature range. The angular variation of the gap is shown in the *inset(a)* in Fig. 5. A hypothetical nodal case with  $r = 1.2$  is shown for comparison. For the fitting, the temperature - dependent part of the gap,  $\Psi(t)$ , was calculated self-consistently [14] and is shown in *inset(b)* in comparison with the isotropic case of  $r = 0$ .

For completeness, we also used self-consistent two-gap  $\gamma$ -model [54] as shown by the dashed line in Fig. 5, but being isotropic, it only captures the intermediate temperatures. Nevertheless, the interaction parameters inferred from the  $\gamma$ -model fitting result in a positive average of the interaction matrix,  $\langle V \rangle > 0$ , which is important for the discussion below.

### DISCUSSION: RECONCILING LOW- $T$ PAIRBREAKING EFFECTS WITH $T_c$ ENHANCEMENT BY IRRADIATION

It is clearly important to try to reconcile data at low temperatures, including the small gap and its enhancement with electron irradiation – all consistent with pair-breaking in an anisotropic  $s$ -wave state – with the remarkable fact that  $T_c$  *increases* with irradiation. Note that there are several examples in the literature where irradiation – for example by heavy ions – produces essentially no change in  $T_c$ . These effects have been understood in terms of mesoscopic inhomogeneity, in contrast to the spatially uniform disorder produced at the

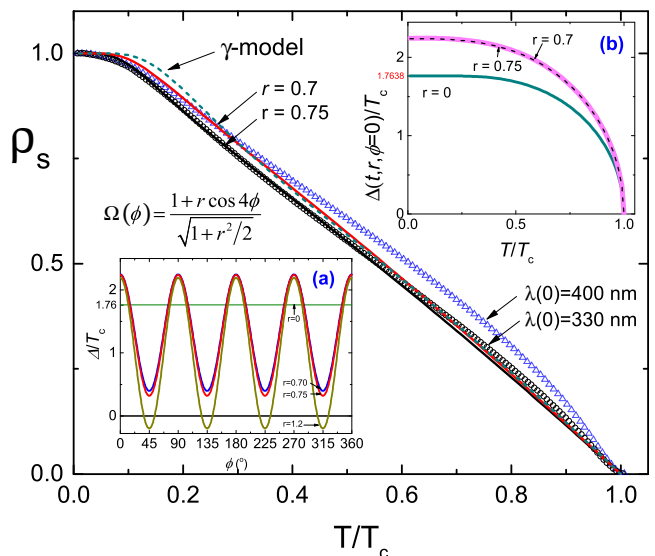


FIG. 5. (Color online) Superfluid density analyzed in terms of anisotropic gap in the form shown. The best fit is obtained for  $\rho_s$  calculated with  $\lambda(0) = 330$  nm, but  $\rho_s$  with  $\lambda(0) = 400$  nm can also be fitted at  $t < 0.3$ . For completeness, a two-gap  $\gamma$ -model[54] fit is shown by the dashed line. *Inset (a)* angular variation of the gap with  $r = 0.70$  (best fit of  $\lambda(0) = 400$  nm data),  $r = 0.75$  (best fit of  $\lambda(0) = 330$  nm data) and  $r = 1.2$  of the hypothetical accidental nodes state. *Inset (b)* shows variation of the gap with temperature, obtained from the self-consistency equation.

nanoscale by electron irradiation. In pnictides, however, e.g. the  $\text{BaFe}_2\text{As}_2$ -based “Ba122” compounds,  $T_c$  is suppressed fairly rapidly by 2.5 MeV electron irradiation [6, 9]. For example, in  $\text{BaFe}_2(\text{As}_{0.67}\text{P}_{0.33})_2$ , essentially the same irradiation dosage applied in this work produced a suppression of 5% of  $T_c$ , whereas in  $\text{FeSe}$   $T_c$  increases by about the same amount. This effect is therefore qualitatively different. Some aspects of the defects created by electron irradiation in this system are therefore not consistent with a purely pairbreaking interpretation, but may effectively dope the system, exert chemical pressure, or by some other means enhance the pairing interaction (“*pair strengthening*”). Another possibility is if superconductivity in  $\text{FeSe}$  is competing with a secondary order that is suppressed more rapidly by disorder than superconductivity itself; this is analogous to the mechanism proposed for enhancement of  $T_c$  by disorder in the spin density wave phase of the  $\text{Ba}(\text{Fe}_{1-x}\text{Co}_x)_2\text{As}_2$  system [10, 55] by Fernandes *et al.* [4].

Assuming that whatever effect leads to  $T_c$  enhancement is rather small, one may ask, how is it able to overcome the pairbreaking effect of disorder? There are several situations in which pairbreaking, even in a highly anisotropic superconductor, is fairly minimal. The first example is a conventional non-sign-changing “ $s_{++}$ ” superconductor, where nonmagnetic disorder is pair-breaking only to the extent that it averages the gap



anisotropy [56]. This seems unlikely simply because the electronic interactions and Fermi surface of FeSe are so similar to the Fe-pnictides, where there is considerable experimental evidence and theoretical justification for an  $s_{\pm}$  identification[18]. The second is an “intraband”  $s_{\pm}$  superconductor, which behaves nearly equivalently to “ $s_{++}$ ” in terms of non-magnetic scattering [3]. Here also, one would have to assume attractive intraband interactions due, presumably, to phonons, leading to a picture quite different from the other systems. Finally, any sort of  $s_{\pm}$  pairing is fairly insensitive to disorder, at least as insensitive as the corresponding anisotropic  $s_{++}$  state, provided the disorder scattering is primarily intraband in nature. It seems to us that this latter possibility is likely to be the case. If we compare to the example given above, of electron irradiated  $\text{BaFe}_2(\text{As}_{0.67}\text{P}_{0.33})_2$ , then the effect of pair strengthening or competing order would have to be of roughly the same order but a bit larger compared to the (opposite sign) effect of disorder pairbreaking.

Of the various scenarios considered to enhance  $T_c$ , some seem unlikely. For example, we measured Hall coefficient in BaK122 crystals of different doping levels and with different doses, and found that that electron irradiation is not doping the system [57]. Enhancement of  $T_c$  by the suppression of competing order by impurity scattering relies on a scenario whereby the competing order is more sensitive to the disorder than the superconductivity itself. For example, in the case discussed by Fernandes *et al.* [4],  $(\pi, 0)$  stripe order is sensitive to impurity scattering by both  $q = 0$  and  $(\pi, 0)$ , but isotropic  $s_{\pm}$  superconductivity is sensitive only to scattering by  $(\pi, 0)$ .

In FeSe there appears to be no long range magnetic order, but significant nematic order is present due to weak orthorhombic distortion below structural transition. Assuming a competition between the two states appears reasonable because  $T_s$  is suppressed and  $T_c$  enhanced both under hydrostatic pressure and, more recently, sulfur doping [20, 58, 59]. The effect of disorder on these two competing states is however not as straightforward as in the case of  $s_{\pm}$  superconductivity competing with the  $(\pi, 0)$  spin density wave, both because the nematic state is a form of  $q = 0$  order, and because the anisotropic superconducting state is sensitive to small  $q$  as well as large  $q$  scattering. However, it can be shown that a  $d$ -wave Pomeranchuk instability is weakened by point-like impurity scattering [60]. Such a suppression of a  $d$ -wave Pomeranchuk state is also expected in accordance with Imry-Ma theorem [61]. Since  $d$ -wave Pomeranchuk order leads to deformation of the Fermi surface, it can strongly suppress superconductivity. If nematic order in FeSe is of this general type, we may expect that as it deteriorates due to disorder, superconductivity will get a boost, which under some circumstances may overcome the pairbreaking damage done by the disorder. Further work is needed to establish this scenario in context of

multiband Fe-based superconductors.

For completeness, we mention that the nematic phase of FeSe has been interpreted in terms of various quadrupolar magnetic “hidden” long range orders[62, 63], which may be quite sensitive to disorder. Thus far neither this sensitivity nor the competition with superconductivity has addressed in the literature.

We now consider the possibility that the Frenkel pairs created by electron irradiation change the lattice in a way that mimics some kind of chemical pressure, thereby altering the electronic structure and thereby the pairing interaction itself subtly. One effect of this type is of course actual hydrostatic pressure, where  $T_c$  is observed to increase simultaneously with the decrease of  $T_s$ , exactly as observed here. On the other hand, the creation of Frenkel defects should expand rather than collapse the lattice. Nevertheless, similar effects have been seen when the lattice is expanded, e.g., in the FeSe intercalate family. As pointed out by Noji *et al.* [64], expanding the lattice in the  $c$ -direction in the range of 5-9 Å increases  $T_c$  linearly at a rate of about 14 K/Å. FeSe itself is at the bottom of this lattice constant range. This trend in the intercalates was reproduced by spin fluctuation theory with the calculated Fermi surfaces as input[65], and arises crudely due to the increase of the Fermi level density of states as  $c$  increases. On the other hand, uniaxial thermal-expansion measurements show, via thermodynamic relations, that  $T_c$  is mostly affected by the in-plane lattice parameters,  $a$  and  $b$ , and is much less sensitive to the  $c$ -axis lattice constant [48]. In either case, our estimates of the average stretch of the  $c$ -axis lattice constant with irradiation provide an effect that is an order of magnitude too small to influence  $T_c$  via chemical pressure mechanism compared to the 5% enhancement observed. With our irradiation dose, we create approximately  $3.6 \times 10^{-3}$  Frenkel pairs per unit cell and even most optimistic estimates give a minuscule volume change,  $\Delta V/V_0 < 10^{-3}$ , which at best can result in about 0.1 K change of  $T_c$  for any optimistic scenario of either expansion of the  $c$ -axis [64] or hydrostatic pressure. Furthermore, upon warming up to room temperature about 30 % of Frenkel pairs recombine as was directly determined from *in-situ* resistivity measurements [6] and it is also believed that most interstitials will migrate from sample interior to surfaces, dislocations and other “sinks” in the crystal [66, 67]. This will make the above estimates even lower and we may safely conclude that pressure due to electron irradiation cannot explain our results.

This leaves us with the very plausible possibility that the impurity is pair strengthening, i.e. that it enhances the pair interaction locally, as discussed in several microscopic models [68–71]. Here the basic idea is that the electronic structure is modulated locally so that it enhances the magnetic exchange in the strong coupling limit, or drives the system closer to a local Stoner instability, in the weak coupling case. Note that the impurity can at

the same time possess an electrostatic potential component that is itself pair breaking; the competition between these two effects decides whether  $T_c$  is enhanced locally or not. As discussed in *Supplementary Information*, for the concentration of defects estimated in our irradiated sample, the defects are on the average well within a coherence length of one another, so there is a percolating superconducting path at the enhanced  $T_c$ , such that it can be detected in transport. The broadening of the transition by irradiation tends to support an inhomogeneous enhancement of this type. Note that since the above theoretical works considered only Hubbard-type 1-band models, considerable further work is necessary to establish the validity of this scenario in the context of the Fe-based materials.

### The role of twins

The observation of small gaps at low temperatures in some samples may also be due to differences in sample growth, preparation and mounting for measurements that introduce different amounts of strain, and hence result in higher density of twins below the structural transition in some samples. Since twins appear to promote nodeless over nodal behavior[45] and the effect is long-range, samples with higher twin density may display predominantly nodeless gaps. It is interesting to note in this context that the difference in resistivity between the nodal samples of Kasahara *et al.* and other samples (ours including) are mostly visible below the structural transition where twins form [25].

### CONCLUSIONS

We have performed penetration depth measurements down to low temperatures on pristine and electron-irradiated samples of FeSe. In both samples, the low- $T$  variation of  $\Delta\lambda$  is consistent with a small minimum gap, which increases from 0.7 K in the pristine sample to 1.3K in the irradiated sample, suggesting the effect of gap averaging by disorder. There are now reports in the literature claiming both nodal and small full gaps in FeSe crystals, and it will be important to establish whether the full gap samples are dirtier or cleaner. Thus far, our results with a single irradiation dose suggest that the gap opens with disorder, hence we expect the nodal samples are cleaner. Our findings of the small gap are consistent with a highly anisotropic gap function, either of  $s_{++}$  or  $s_{+/-}$  character, provided in the latter case disorder is of a sufficiently intraband character, so that  $T_c$  suppression is small.

At higher temperatures, we found that irradiation decreased the structural transition  $T_s$  by 0.9K, but surprisingly,  $T_c$  was *enhanced* in the same sample by 0.4K, nearly

5% of  $T_c$ . We discussed several theoretical scenarios that might account for the latter effect, and concluded that a local pair strengthening by irradiation-induced Frenkel defects, which locally enhance spin fluctuations near a magnetic transition, is the most likely explanation.

### ACKNOWLEDGEMENTS

We thank A. Chubukov, B. Andersen, A. Golubov, R. Fernandes, M. Iavarone, S. Maiti, Y. Matsuda, I. Mazin, S. Roessler, T. Shibauchi, and L. Taillefer for useful discussions. We are particularly grateful to S. Røßler for drawing our attention to the effects of twins on the resistivity and to M. Kończykowski as well as the whole SIRIUS team, B. Boizot, V. Metayer, and J. Losco, for running electron irradiation at *École Polytechnique*.

This work was supported by the U.S. Department of Energy (DOE), Office of Science, Basic Energy Sciences, Materials Science and Engineering Division. Ames Laboratory is operated for the U.S. DOE by Iowa State University under contract DE-AC02-07CH11358. Electron irradiation was supported by EMIR network, proposal 11-11-0121. VM acknowledges the support from the Laboratory Directed Research and Development Program of Oak Ridge National Laboratory, managed by UT-Battelle, LLC, for the U. S. Department of Energy. PJH was partially supported by NSF-DMR-1005625. A. E. B. acknowledges support from the Helmholtz Association via PD-226.

---

\* Corresponding author: prozorov@ameslab.gov

- [1] P. J. Hirschfeld and N. Goldenfeld, Phys. Rev. B **48**, 4219 (1993).
- [2] R. Prozorov and R. W. Giannetta, Supercond. Sci. Technol. **19**, R41 (2006).
- [3] D. V. Efremov, M. M. Korshunov, O. V. Dolgov, A. A. Golubov, and P. J. Hirschfeld, Phys. Rev. B **84**, 180512 (2011).
- [4] R. M. Fernandes, M. G. Vavilov, and A. V. Chubukov, Phys. Rev. B **85**, 140512 (2012).
- [5] Y. Wang, A. Kreisel, P. J. Hirschfeld, and V. Mishra, Phys. Rev. B **87**, 094504 (2013).
- [6] R. Prozorov, M. Konczykowski, M. A. Tanatar, A. Thaler, S. L. Bud'ko, P. C. Canfield, V. Mishra, and P. J. Hirschfeld, Phys. Rev. X **4**, 041032 (2014).
- [7] C. P. Strehlow, M. Konczykowski, J. A. Murphy, S. Teknowijoyo, K. Cho, M. A. Tanatar, T. Kobayashi, S. Miyasaka, S. Tajima, and R. Prozorov, Phys. Rev. B **90**, 020508 (2014).
- [8] K. Cho, M. Konczykowski, J. Murphy, H. Kim, M. A. Tanatar, W. E. Straszheim, B. Shen, H. H. Wen, and R. Prozorov, Phys. Rev. B **90**, 104514 (2014).
- [9] Y. Mizukami, M. Konczykowski, Y. Kawamoto, S. Kurata, S. Kasahara, K. Hashimoto, V. Mishra, A. Kreisel,

- Y. Wang, P. J. Hirschfeld, Y. Matsuda, and T. Shibauchi, *Nat. Comm.* **5**, 5657 (2014).
- [10] P. C. Canfield and S. L. Bud'ko, *Annual Review of Condensed Matter Physics* **1**, 27 (2010).
- [11] I. I. Mazin, *Nature* **464**, 183 (2010).
- [12] D. C. Johnston, *Adv. Phys.* **59**, 803 (2010).
- [13] J. Paglione and R. Greene, *Nat. Phys.* **6**, 645 (2010).
- [14] R. Prozorov and V. G. Kogan, *Rep. Prog. Phys.* **74**, 124505 (2011).
- [15] G. R. Stewart, *Rev. Mod. Phys.* **83**, 1589 (2011).
- [16] A. Chubukov, *Ann. Rev. Cond. Mat. Phys.* **3**, 57 (2012).
- [17] A. Chubukov and P. J. Hirschfeld, *Phys. Today* **68**, 46 (2015).
- [18] P. J. Hirschfeld, *C. R. Phys.* **17**, 197 (2016).
- [19] R. M. Fernandes and J. Schmalian, *Phys. Rev. B* **82** (2010).
- [20] Y. Mizuguchi and Y. Takano, *J. Phys. Soc. Japan* **79**, 102001 (2010).
- [21] A. Subedi, L. Zhang, D. J. Singh, and M. H. Du, *Phys. Rev. B* **78**, 134514 (2008).
- [22] V. G. Kogan, *Phys. Rev. B* **80**, 214532 (2009).
- [23] R. T. Gordon, H. Kim, M. A. Tanatar, R. Prozorov, and V. G. Kogan, *Phys. Rev. B* **81**, 180501 (2010).
- [24] K. Miyoshi, K. Morishita, E. Mutou, M. Kondo, O. Seida, K. Fujiwara, J. Takeuchi, and S. Nishigori, *J. Phys. Soc. Japan* **83**, 013702 (2014).
- [25] S. Knöner, D. Zielke, S. Köhler, B. Wolf, T. Wolf, L. Wang, A. Böhrer, C. Meingast, and M. Lang, *Phys. Rev. B* **91**, 174510 (2015).
- [26] U. S. Kaluarachchi, V. Taufour, A. E. Böhrer, M. A. Tanatar, S. L. Bud'ko, V. G. Kogan, R. Prozorov, and P. C. Canfield, *Phys. Rev. B* **93**, 064503 (2016).
- [27] F. Wang, S. A. Kivelson, and D.-H. Lee, *Nature Physics* **11**, 959 (2015).
- [28] J. K. Glasbrenner, I. I. Mazin, H. O. Jeschke, P. J. Hirschfeld, R. M. Fernandes, and R. Valenti, *Nat. Phys.* **11**, 953 (2015), article.
- [29] Y. Yamakawa, S. Onari, and H. Kontani, (2015).
- [30] A. V. Chubukov, M. Khodas, and R. M. Fernandes, *ArXiv e-prints* (2016).
- [31] M. A. Tanatar, A. E. Bohmer, E. I. Timmons, M. Schutt, G. Drachuck, V. Taufour, S. L. Budko, P. C. Canfield, R. M. Fernandes, and R. Prozorov, *arXiv:1511.04757* (2015).
- [32] D. Liu, W. Zhang, D. Mou, J. He, Y.-B. Ou, Q.-Y. Wang, Z. Li, L. Wang, L. Zhao, S. He, Y. Peng, X. Liu, C. Chen, L. Yu, G. Liu, X. Dong, J. Zhang, C. Chen, Z. Xu, J. Hu, X. Chen, X. Ma, Q. Xue, and X. Zhou, *Nat Commun* **3**, 931 (2012).
- [33] S. He, J. He, W. Zhang, L. Zhao, D. Liu, X. Liu, D. Mou, Y.-B. Ou, Q.-Y. Wang, Z. Li, L. Wang, Y. Peng, Y. Liu, C. Chen, L. Yu, G. Liu, X. Dong, J. Zhang, C. Chen, Z. Xu, X. Chen, X. Ma, Q. Xue, and X. J. Zhou, *Nat. Mater.* **12**, 605 (2013), letter.
- [34] S. Kasahara, T. Watashige, T. Hanaguri, Y. Kohsaka, T. Yamashita, Y. Shimoyama, Y. Mizukami, R. Endo, H. Ikeda, K. Aoyama, T. Terashima, S. Uji, T. Wolf, H. von Löhneysen, T. Shibauchi, and Y. Matsuda, *Proceedings of the National Academy of Sciences* **111**, 16309 (2014).
- [35] T. Terashima, N. Kikugawa, A. Kiswandhi, E.-S. Choi, J. S. Brooks, S. Kasahara, T. Watashige, H. Ikeda, T. Shibauchi, Y. Matsuda, T. Wolf, A. E. Böhrer, F. Hardy, C. Meingast, H. v. Löhneysen, M.-T. Suzuki, R. Arita, and S. Uji, *Phys. Rev. B* **90**, 144517 (2014).
- [36] P. Choubey, T. Berlijn, A. Kreisel, C. Cao, and P. J. Hirschfeld, *Phys. Rev. B* **90**, 134520 (2014).
- [37] A. Kreisel, S. Mukherjee, P. J. Hirschfeld, and B. M. Andersen, *Phys. Rev. B* **92**, 224515 (2015).
- [38] S. Mukherjee, A. Kreisel, P. J. Hirschfeld, and B. M. Andersen, *Phys. Rev. Lett.* **115**, 026402 (2015).
- [39] C.-L. Song, Y.-L. Wang, P. Cheng, Y.-P. Jiang, W. Li, T. Zhang, Z. Li, K. He, L. Wang, J.-F. Jia, H.-H. Hung, C. Wu, X. Ma, X. Chen, and Q.-K. Xue, *Science* **332**, 1410 (2011).
- [40] M. Abdel-Hafez, J. Ge, A. N. Vasiliev, D. A. Chareev, J. Van de Vondel, V. V. Moshchalkov, and A. V. Silhanek, *Phys. Rev. B* **88**, 174512 (2013).
- [41] J.-Y. Lin, Y. S. Hsieh, D. A. Chareev, A. N. Vasiliev, Y. Parsons, and H. D. Yang, *Phys. Rev. B* **84**, 220507 (2011).
- [42] L. Jiao, C.-L. Huang, S. Röler, C. Koz, U. K. Röler, U. Schwarz, and S. Wirth, *Arxiv:1605.01908* (2016).
- [43] J. K. Dong, T. Y. Guan, S. Y. Zhou, X. Qiu, L. Ding, C. Zhang, U. Patel, Z. L. Xiao, and S. Y. Li, *Phys. Rev. B* **80**, 024518 (2009).
- [44] P. Bourgeois-Hope, S. Chi, D. A. Bonn, R. Liang, W. N. Hardy, T. Wolf, C. Meingast, N. Doiron-Leyraud, and L. Taillefer, *arXiv:1603.06917* (2016).
- [45] T. Watashige, Y. Tsutsumi, T. Hanaguri, Y. Kohsaka, S. Kasahara, A. Furusaki, M. Sigrist, C. Meingast, T. Wolf, H. v. Löhneysen, T. Shibauchi, and Y. Matsuda, *Phys. Rev. X* **5**, 031022 (2015).
- [46] X. Liu, L. Zhao, S. He, J. He, D. Liu, D. Mou, B. Shen, Y. Hu, J. Huang, and X. J. Zhou, *Journal of Physics: Condensed Matter* **27**, 183201 (2015).
- [47] Y. Dongna, Y. Jie, H. Yulong, N. Shunli, F. Zhongpei, Z. Huaxue, M. Yiyuan, J. Kui, Z. Guangming, D. Xiaoli, Z. Fang, and Z. Zhongxian, (2016), 1605.01507.
- [48] A. E. Böhrer, F. Hardy, F. Eilers, D. Ernst, P. Adelman, P. Schweiss, T. Wolf, and C. Meingast, *Phys. Rev. B* **87**, 180505 (2013).
- [49] R. Prozorov, R. W. Giannetta, A. Carrington, and F. M. Araujo-Moreira, *Phys. Rev. B* **62**, 115 (2000).
- [50] K. Kothapalli, A. E. Böhrer, W. T. Jayasekara, B. G. Ueland, P. Das, A. Sapkota, V. Taufour, Y. Xiao, E. E. Alp, S. L. Bud'ko, P. C. Canfield, A. Kreyssig, and A. I. Goldman, *ArXiv:1603.04135* (2016).
- [51] <http://emir.in2p3.fr/LSI>.
- [52] Note that because our samples are twinned [31], the supercurrent flows through structural domains of both orientations. In principle, if one orientation is nodal, we should detect it in the clean limit.
- [53] V. Mishra, G. Boyd, S. Graser, T. Maier, P. J. Hirschfeld, and D. J. Scalapino, *Phys. Rev. B* **79**, 094512 (2009).
- [54] V. G. Kogan, C. Martin, and R. Prozorov, *Phys. Rev. B* **80**, 014507 (2009).
- [55] N. Ni, A. Thaler, J. Q. Yan, A. Kracher, E. Colombier, S. L. Bud'ko, P. C. Canfield, and S. T. Hannahs, *Phys. Rev. B* **82**, 024519 (2010).
- [56] D. Markowitz and L. P. Kadanoff, *Phys. Rev.* **131**, 563 (1963).
- [57] R. Prozorov, M. Konczykowski, M. A. Tanatar, B. Shen, H.-H. Wen, I. I. Mazin, and R. M. Fernandes, to be published (2016).
- [58] Y. Mizuguchi, F. Tomioka, S. Tsuda, T. Yamaguchi, and Y. Takano, *J. Phys. Soc. Japan* **78**, 074712 (2009).
- [59] M. D. Watson, T. K. Kim, A. A. Haghighirad, S. F.



- Blake, N. R. Davies, M. Hoesch, T. Wolf, and A. I. Coldea, Phys. Rev. B **92**, 121108 (2015).
- [60] A. F. Ho and A. J. Schofield, EPL (Europhysics Letters) **84**, 27007 (2008).
  - [61] Y. Imry and S.-k. Ma, Phys. Rev. Lett. **35**, 1399 (1975).
  - [62] R. Yu and Q. Si, Phys. Rev. Lett. **115**, 116401 (2015).
  - [63] Z. Wang, W.-J. Hu, and A. H. Nevidomskyy, ArXiv e-prints (2016).
  - [64] T. Noji, T. Hatakeda, S. Hosono, T. Kawamata, M. Kato, and Y. Koike, Physica C **504**, 8 (2014).
  - [65] D. Guterding, H. O. Jeschke, P. J. Hirschfeld, and R. Valentí, Phys. Rev. B **91**, 041112 (2015).
  - [66] A. C. Damask and G. J. Dienes, *Point Defects in Metals* (Gordon & Breach Science Publishers Ltd, 1963) iSBN-13: 9780677001906 iSBN-10: 0677001908.
  - [67] M. W. Thompson, *Defects and Radiation Damage in Metals*, revised september 27, 1974 ed., Cambridge Monographs on Physics (Cambridge University Press, 1969) iSBN-13: 978-0521098656, iSBN-10: 0521098653.
  - [68] T. S. Nunner, B. M. Andersen, A. Melikyan, and P. J. Hirschfeld, Phys. Rev. Lett. **95**, 177003 (2005).
  - [69] M. M. Maška, i. d. Z. Śledź, K. Czajka, and M. Mierzejewski, Phys. Rev. Lett. **99**, 147006 (2007).
  - [70] K. Foyevtsova, R. Valentí, and P. J. Hirschfeld, Phys. Rev. B **79**, 144424 (2009).
  - [71] A. T. Rømer, S. Graser, T. S. Nunner, P. J. Hirschfeld, and B. M. Andersen, Phys. Rev. B **86**, 054507 (2012).
  - [72] “Calculations of cross - sections by electron irradiation according to O. S. Oen (1965, 1973). C code by Daniel Lesueur, restored by François Beuneu. Ecole Polytechnique, Palaiseau, France,” (1973).

## Supplementary Information

## ELECTRON IRRADIATION

We measure the total dose of electron irradiation in  $\text{C}/\text{cm}^2$  by counting the total charge that passed through a unit area. Therefore,  $1 \text{ C}/\text{cm}^2$  corresponds to  $6.24 \times 10^{18}$  electrons per  $\text{cm}^2$ . In this work we accumulated  $1.8 \text{ C}/\text{cm}^2$  or  $1.12 \times 10^{19} e^-/\text{cm}^2$ .

Figure S1 shows ion - specific cross - sections calculated by using the SECTE simulation package [72]. Two pairs of curves for Fe (solid lines) and Se (dashed lines) for two values of the displacement energy,  $E_d = 25 \text{ eV}$  (upper curves) and  $30 \text{ eV}$  (lower curves), in the range commonly found in studies of various materials [66, 67].

At the energy of the electrons used in this study,  $2.5 \text{ MeV}$ , an average cross-section of  $80 \text{ barn}$  will result in generation of  $0.05 \text{ at.}\%$  of Frenkel pairs for ions of each kind per  $1 \text{ C}/\text{cm}^2$  of irradiation dose or  $0.1 \text{ at.}\%$  of defects of either kind per formula or, with  $Z=2$  of  $\text{FeSe}$ ,  $0.2 \text{ at.}\%$  of defects of either kind per unit cell.

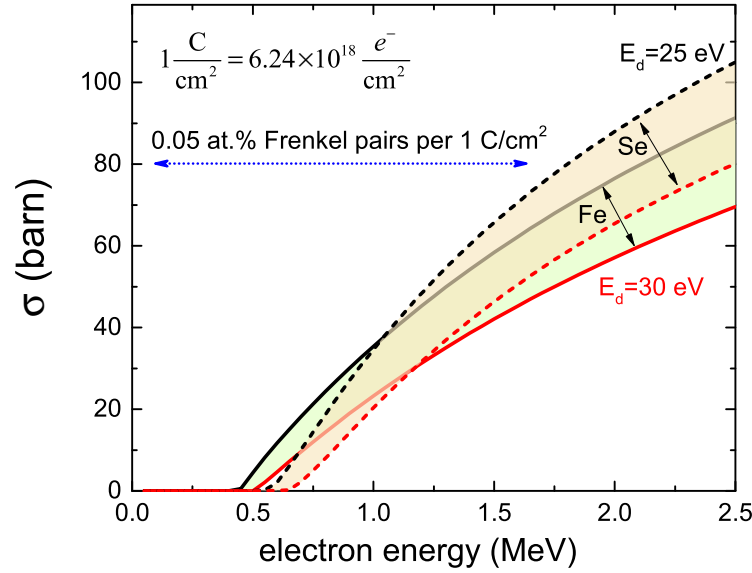


FIG. S1. (Color online) Ion - specific cross-sections calculated by using SECTE program. The upper curves correspond to the ion knock-out threshold of  $E_d = 25 \text{ eV}$ , the lower curves to  $E_d = 30 \text{ eV}$ . Se is shown by dashed curves, Fe by solid curves. At a mid-range value of  $80 \text{ barn}$ , we expect  $0.05 \text{ at.}\%$  per ion type of the Frenkel pairs per formula.

It is instructive to compare the average distance between the defects with the coherence length. A unit cell volume of  $\text{FeSe}$  is  $78.4 \text{ \AA}^3$ . With  $Z=2$ , we have for  $1.8 \text{ C}/\text{cm}^2$ ,  $2 \times 1.8 \times 1 \times 10^{-3} = 0.0036$  Frenkel pairs of either Fe or Se per unit volume. Therefore, a volume that will contain at least one Frenkel pair is  $78.4/0.0036 = 2.1 \times 10^4 \text{ \AA}^3$ , so that the average distance between these defects is  $(2.1 \times 10^4)^{1/3} \approx 30 \text{ \AA}$ . (Taking into account annealing of the defects upon warming up does not change this number much due to  $1/3$  power.) This should be compared to the coherence length, which we can evaluate from the upper critical fields. Along the  $c$ -axis,  $H_{c2,c} \approx 17 \text{ T}$  and along the  $ab$ -plane it is about  $30 \text{ T}$  [35]. This gives coherence lengths of  $\xi_{ab} = 110 \text{ \AA}$  and  $\xi_c = 83 \text{ \AA}$ , respectively. Terashima *et al.* estimate the coherence lengths from the slope of  $dH_{c2}/dT$  at  $130 \text{ \AA}$  and  $57 \text{ \AA}$ , which is, indeed, close to our estimate. In either case, these coherence lengths are larger than the distance between the defects of  $30 \text{ \AA}$  and, therefore, according to Markowitz and Kadanoff  $T_c$  suppression should saturate as function of scattering [56].

## SUPERFLUID DENSITY OF TWO SAMPLES BEFORE AND AFTER IRRADIATION

In order to calculate superfluid density,  $\rho_s = (1 + \Delta\lambda(T)/\lambda(0))^{-2}$ , from our data we need to know the absolute value of the London penetration depth,  $\lambda(0)$ . In Fig. S2, the superfluid density  $\rho(t)$  is plotted with  $\lambda(0) = 400 \text{ nm}$  obtained from microwave cavity perturbation measurements of similar  $\text{FeSe}$  crystals [34]. Saturation at  $T \rightarrow 0$  can be clearly seen below approximately  $0.5T/T_c$  (as opposite to  $0.3T/T_c$  of the isotropic  $s$ -wave shown by grey line). An overall shape of  $\rho_s(T)$  indicates a large number of thermally excited quasiparticles at the elevated temperatures

compared to the expectations of the isotropic gap and not too far from the nodal  $d$ -wave line, but only at elevated temperatures. After electron irradiation, the superfluid density decreases even more departing significantly from the pristine samples. However, most likely  $\lambda(0)$  increases, which will reduce the difference.

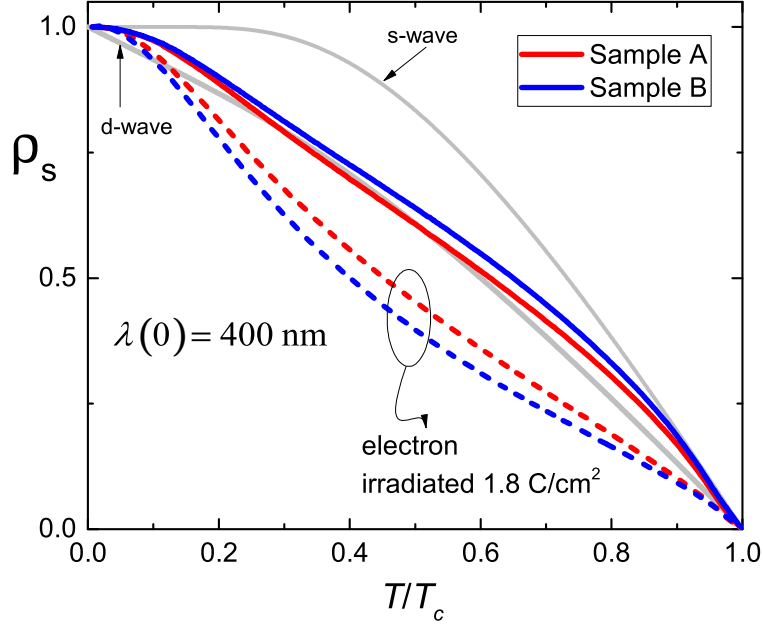


FIG. S2. (Color online) Superfluid density  $\rho_s(t)$  before (solid lines) and after (dashed lines)  $1.8 \text{ C/cm}^2$   $2.5 \text{ MeV}$  electron irradiation for samples A and B. Solid grey lines show standard  $s$ - and  $d$ - wave curves for comparison.  $\lambda(0) = 400 \text{ nm}$  was assumed.

### ANISOTROPIC $s$ -WAVE GAP WITH NODES

We use a commonly - used ansatz of temperature and angle separation [22],

$$\Delta(T, \phi) = \Psi(T)\Omega(\phi), \quad \langle \Omega^2 \rangle_{FS} = 1 \quad (\text{S1})$$

Here we specifically use the form of the angular part of the gap commonly used to describe iron pnictides- based superconductors [16–18],

$$\Omega(\phi) = \frac{1 + r \cos 4\phi}{\sqrt{1 + r^2/2}} \quad (\text{S2})$$

and self-consistency equation for the temperature - dependent part,  $\Psi(T)$ , (see Eq. (20) in Ref. [14]),

$$\frac{1}{2\pi T} \ln \frac{T_c}{T} = \sum_{\omega > 0}^{\infty} \left( \frac{1}{\hbar\omega} - \left\langle \frac{\Omega^2}{\sqrt{\Psi^2 \Omega^2 + \hbar^2 \omega^2}} \right\rangle_{FS} \right). \quad (\text{S3})$$

where  $\hbar\omega = \pi k_B T(2n + 1)$  are the Matsubara frequencies. Fitting of the experimental superfluid density using Eqs. (S1), (S2) and (S3) is shown in Fig. 5, where *inset(a)* shows the angular part,  $\Omega(\phi)$  and *inset(b)* shows self-consistent solutions for the gap, using Eq. (S3).

Figure S3 shows an interesting results of *non-monotonic*  $r$ - dependence of the  $\Delta(t = 0, r, \phi = 0)/T_c$ , obtained self-consistently from Eq. (S3). While by itself it does not imply non-monotonic  $T_c$ , further microscopic analysis would be of interest.

Finally, the Abrikosov-Gorkov theory generalized to arbitrary  $\Omega(\phi)$  (Born limit and isotropic scattering) reads [22],

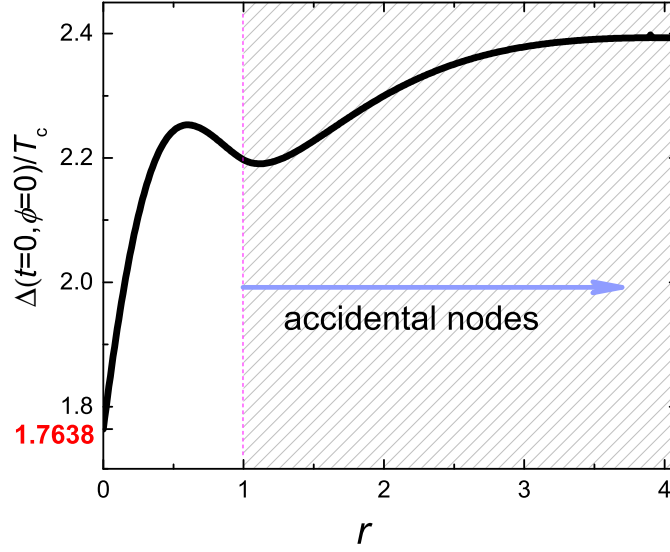


FIG. S3. (Color online)  $\Delta(t=0, r, \phi=0)/T_c$  vs  $r$ , where  $\Delta(t, r, \phi) = \Psi(t)\Omega(r, \phi)$  and  $\Psi(t)$  is the solution of self-consistency equation, Eq. S3.

$$-\ln t_c = \psi\left(\frac{1}{2} + \frac{g+g_m}{2t_c}\right) - \psi\left(\frac{1}{2}\right) - \langle \Omega \rangle^2 \left( \psi\left(\frac{1}{2} + \frac{g+g_m}{2t_c}\right) - \psi\left(\frac{1}{2} + \frac{g_m}{2t_c}\right) \right) \quad (\text{S4})$$

where  $\psi$  is the digamma function,  $t_c = T_c/T_{c0}$  and normalized non-magnetic,  $g = \hbar/(2\pi k_B T_{c0} \tau)$ , and magnetic,  $g_m = \hbar/(2\pi k_B T_{c0} \tau_m)$  scattering rates with  $\tau$  and  $\tau_m$  being potential and spin-flip scattering times, respectively. In our case of  $\Omega(\phi)$  given by Eq. (S2), therefore  $\langle \Omega \rangle^2 = 2/(2+r^2)$  for a cylindrical Fermi surface.

Solutions of Eq.(S4) with  $g_m=0$  and  $\Omega$  given by Eq. (S2) for different values of  $r$  are shown in Fig. S4.

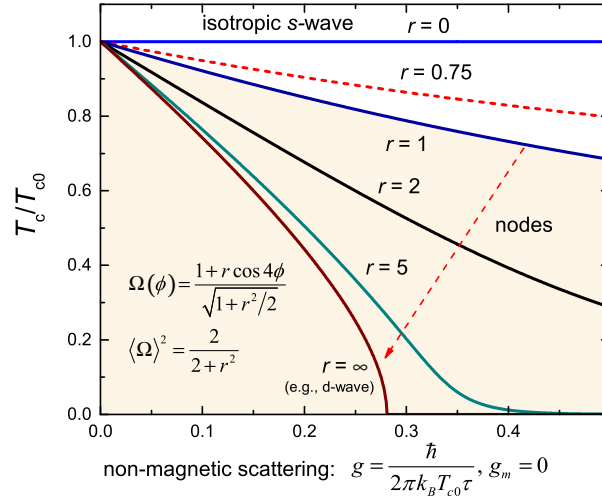


FIG. S4. (Color online) Suppression of the transition temperature,  $T_c/T_{c0}$ , versus non-magnetic scattering rate,  $g$ , for several values of the anisotropy amplitude,  $r$ . At  $r=0$  the gap is isotropic and accidental nodes appear for  $r \geq 1$ . Best fit to our data, Fig. 5, is obtained with  $r=0.75$  (red dashed line).  $d$ -wave state is shown for comparison.